Computers and Concrete, *Vol. 15, No. 2 (2015) 199-213*
DOI: http://dx.doi.org/10.12989/cac.2015.15.2.199

Influence of softening curves on the residual fracture toughness of post-fire normal-strength concrete

Kequan YU* and Zhoudao LU[a]

College of civil engineering, Tongji University, No.1239 SiPing Road, Shanghai, China

(*Received April 10, 2013, Revised December 29, 2014, Accepted January 3, 2015*)

Abstract. The residual fracture toughness of post-fire normal-strength concrete subjected up to 600℃ is considered by the wedge splitting test. The initial fracture toughness K_I^{ini} and the critical fracture toughness K_I^{un} could be calculated experimentally. Their difference is donated as the cohesive fracture toughness K_I^c which is caused by the distribution of cohesive stress on the fracture process zone. A comparative study on determining the residual fracture toughness associated with three bi-linear functions of the cohesive stress distribution, i.e. Peterson's softening curve, CEB-FIP Model 1990 softening curve and Xu's softening curve, using an analytical method is presented. It shows that different softening curves have no significant influence on the fracture toughness. Meanwhile, comparisons between the experimental and the analytical calculated critical fracture toughness values further prove the validation of the double-K fracture model to the post-fire concrete specimens.

Keywords: post-fire; fracture toughness; bi-linear; softening curve; double-K fracture model

Nomenclature

a	equivalent-elastic crack length, m	a_c	critical notch depth of the specimen, m
a_s	effective crack length corresponding to w_s, m	a_0	initial notch depth of the specimen, m
$CMOD$	crack mouth opening displacement, mm	$CMOD$	critical crack mouth opening displacement, mm
$CTOD$	crack tip opening displacement, mm	$CTOD_c$	critical crack tip opening displacement, mm
d_{max}	maximum diameter of coarse aggregate, mm	E	residual Young's modulus , MPa
f_t	tensile strength, MPa	G_F	fracture energy, N/m
h	height of wedge splitting specimens, mm	h_0	thickness of the clip gauge holder, mm
K_I^{ini}	initial fracture toughness, MN/m$^{1.5}$	$K_I^{un\text{-}E}$	experimental unstable fracture toughness, MN/m$^{1.5}$
$K_I^{un\text{-}A}$	analytical unstable fracture toughness, MN/m$^{1.5}$	$K_I^{c\text{-}A}$	cohesive fracture toughness by analytical method, MN/m$^{1.5}$
K_I^c	cohesive fracture toughness, MN/m$^{1.5}$	P_{ini}	the initial cracking load , kN

∗Corresponding author, PhD Candidate, E-mail: zjzjykq@163.com
[a]Professor, E-mail: lzd@tongji.edu.cn

Copyright © 2015 Techno-Press, Ltd.
http://www.techno-press.org/?journal=cac&subpage=8 ISSN: 1598-8198 (Print), 1598-818X (Online)

P_{max}	maximum load , kN	T_m	heating temperatures , ℃
w	crack opening displacement at the tip of initial notch, mm	w_s	crack width at break point of softening curve, mm
w_0	crack width at stress-free point, mm	w_u	weight loss of post-fire the specimens, mm
α	coefficient relating to the maximum diameter	$\sigma\,(w)$	cohesive stress at the tip of initial notch , MPa
λ	coefficient relating to the deformation capacity	$\sigma(x)$	cohesive stress at equivalent-elastic crack length x , MPa
$\sigma_s(w_s)$	cohesive stress at the break point of softening curve		

1. Introduction

Since late 1970s, the behavior of crack propagation in quasi-brittle materials like concrete was studied by many researchers (Hillerboerg *et al.*1976, Bazant and Oh 1983, Jenq and shah 1985a, Nallathambi and Karihaloo 1986, Bazant and Kazemi 1990, Xu and Reinhardt 1999a, Kumar and Barai 2008a, b, 2010, 2012). Experimental results showed that the fracture process of concrete structures undergoes three main stages: (i) crack initiation, (ii) stable crack propagation, and (iii) unstable fracture. Accordingly, the double-K fracture criterion showed the crack initiation, crack propagation and failure during a fracture process until the maximum load reached (Xu and Reinhardt 1999a).

Two size-independent parameters, initial cracking toughness, K_I^{ini} and unstable fracture toughness, K_I^{un} can be used to study the crack propagation of concrete. An analytical method (Xu and Reinhardt 1999b) describing the above-mentioned three phases of concrete fracture process was developed using three-point bending test. Using the experimental results Xu and Reinhardt (Xu and Reinhardt 1999c) also showed the validity of double-K fracture criterion on the compact tension specimens and the wedge splitting specimens. In order to determine the double-K fracture parameters analytically, the value of cohesive toughness, K_I^c due to cohesive stress distribution in the fictitious fracture zone should be computed (Jenq and Shah1985b).

Considering there are many structures subjected to fire or high temperatures, the influence of temperature on the fracture properties was considered by several researchers. These researches were mainly on the fracture energy and material brittleness (Bazant and Prat 1988, Baker 1996, Zhang *et al.* 2000, Nielsen and Bicanic 2003, Zhang and Bicanic 2006, Zhang *et al.* 2000a, b, 2002), relatively fewer discussions on the fracture toughness (Prokopski 1995, Hisham and Hamoush 1997). It was found that the residual fracture energy sustained an increase-decease tendency, whereas the residual fracture toughness was greatly influenced by temperatures and decreased steadily. However, in previous research, only the unstable fracture toughness was calculated, neglecting the initial fracture toughness and the relationship between them. Whether the double-K fracture model in ambient temperature was suitable to the post-fire concrete was unknown. Additionally, although in the ambient temperature the concrete softening curve has been extensively investigated (Chen and Su 2013, Bretschneider 2011, Kwon *et al.* 2008, Park *et al.* 2008, Roesler *et al.* 2006), the influence of softening curve on the residual fracture toughness of post-fire concrete was never considered.

In author’s previous work, the residual fracture toughness of wedge splitting specimens subjected to high temperatures was determined and the validation of double-K fracture model to the post-fire concrete was proved (Yu and Lu 2013). Hence, the main concern of this paper is to consider the influence of softening curves on the residual fracture toughness, with which the validation of double-K fracture model could be further proved. The experimental data was from author's previous work (Yu *et al*. 2012), in which the wedge splitting experiments of totally ten temperatures varying from 20℃ to 600℃ and the specimens size 230 mm × 200 mm × 200 mm with initial-notch depth ratio of 0.4 were employed. Hence, the paper is structured as follows: (i) determine the cohesive fracture toughness and the double-K fracture parameters (ii) briefly introduce the experimental work (iii) discuss and compare the influence of softening curve on the fracture toughness.

2. Analytical determination of cohesive fracture toughness

2.1 Effective crack extension length and residual Young's modulus

The linear asymptotic superposition assumption is considered in the analytical method (Xu and Reinhardt 1999b, c) to introduce the concept of linear elastic fracture mechanics for calculating the double-K fracture parameters. Detailed explanation of the above assumption can be found elsewhere (Xu and Reinhardt 1999b). Based on this assumption, the value of the equivalent-elastic crack length for wedge splitting specimen is expressed as:

$$a=(h+h_0)\left(1-\left(\frac{13.18}{E\cdot b\cdot c+9.16}\right)^{1/2}\right)-h_0 \tag{1}$$

where c=$CMOD/P$ is the compliance of specimens, $CMOD$ means the crack opening displacement and P is the corresponding load value; E is the Young's modulus; b is specimens thickness; h is specimens height and h_0 is the thickness of the clip gauge holder. For calculation of critical value of equivalent-elastic crack length a_c, the values of $CMOD$ and P are taken as $CMOD_c$ and P_{max} respectively, which are the critical crack mouth opening displacement and load value.

The residual Young's modulus E is calculated using the P-$CMOD$ curve as:

$$E=\frac{1}{bc_i}\left(13.18\times(1-\alpha)^2-9.16\right) \tag{2}$$

where c_i=$CMOD_{ini}/P_{ini}$ is the initial compliance before cracking, $CMOD_{ini}$ is the initial crack mouth opening displacement, P_{ini} is the initial cracking loading corresponding to $CMOD_{ini}$; α= $(a_0+h_0)/(h+h_0)$, a_0 is the initial notch depth.

The specific values of critical equivalent-elastic crack length a_c and the residual Young's modulus E would be found in elsewhere (Yu and Lu 2014).

2.2 Crack opening displacement along the fracture process zone

Since the cohesive stress distribution along the fracture process zone depends on the crack opening displacement (COD) and the specified softening law, it is important to know the value of COD along the fracture line. It is difficult to measure directly the value of COD along the fracture process zone, for practical purposes the value of $COD(x)$ at the crack length x is computed using the following expression (Jenq and Shah1985a):

$$COD(x) = CMOD\left(\left(1-\frac{x}{a}\right)^2 + \left(1.018-1.149\frac{a}{h}\right)\left(\frac{x}{a}-\left(\frac{x}{a}\right)^2\right)\right)^{1/2} \quad (3)$$

For the calculation of critical crack tip opening displacement $CTOD_c$, the value of x and a (see Fig. 3) in Eq. (3) is taken to be a_o and a_c, respectively. Afterwards, the value of cohesive stress along the fictitious fracture zone to the corresponding crack opening displacement is evaluated using the bilinear stress-displacement softening law as given in Eqs.5-7.

2.3 Determination of stress intensity factor caused by cohesive force

2.3.1 Softening traction-separation law of post-fire concrete

In order to determine the double-K fracture parameters analytically (Xu and Reinhardt 1999b, c) the value of cohesive toughness K_I^c due to cohesive stress distribution in the fictitious fracture zone is computed using the method proposed by Jenq and Shah (Jenq and Shah 1985b). In this method, the determination of K_I^c is done using a special numerical technique because of existence of singularity problem at the integral boundary.

The softening traction-separation law is a prior to determine K_I^c. At room temperature, many expressions have been proposed based on direct tensile tests (Petersson 1981, Gopalaratnam and Shah 1985, Reinhardt *et al.* 1986, Hilsdorf and Brameshuber 1991, Phillips and Zhang 1993). Based on the numerical studies, simplified bilinear expressions for the softening traction-separation law (illustrated in Fig.1) were suggested by Petersson in 1981, Hilsdorft and Brameshuber in 1991, and Phillips and Zhang in 1993. The area under the softening curve was defined as the fracture energy G_F (Hillerboerg *et al*. 1976).

A general form of the simplified bilinear expression of the softening traction-separation law is given as follows:

$$\begin{cases} \sigma = f_t - (f_t - \sigma_s) w/w_0 & 0 \le w \le w_s \\ \sigma = \sigma_s (w_0 - w)/(w_0 - w_s) & w_s \le w \le w_0 \\ \sigma = 0 & w \ge w_0 \end{cases} \quad (4)$$

Different values of the break point (σ_s, w_s) and the crack width w_0 at stress-free point were used for the expression proposed by different researchers. In present work, three bilinear softening functions are listed as follows:

Proposed by Petersson (Petersson 1981)

$$\begin{cases} \sigma_s = f_t / 3 \\ w_s = 0.8 G_F / f_t \\ w_0 = 3.6 G_F / f_t \end{cases} \quad (5)$$

Proposed by CEB-FIP Model Code 1990 (CEB-FIP Model Code 1990):

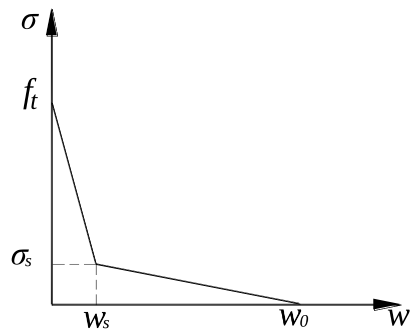

Fig.1. Bilinear softening traction-separation law

$$\begin{cases} \sigma_s = 0.15 f_t \\ w_s = 2G_F / f_t - 0.15 w_0 \\ w_0 = \alpha G_F / f_t \end{cases} \tag{6}$$

where α is a coefficient relating to the maximum diameter of coarse aggregate, α=9-d_{max}/8.

Proposed by Xu (Xu and Reinhardt 1999b):

$$\begin{cases} \sigma_s = \dfrac{f_t}{\alpha}(2 - f_t CTOD_c / G_F) \\ w_s = CTOD_c \\ w_0 = \alpha G_F / f_t \\ \alpha = \lambda - d_{\max} / 8 \end{cases} \tag{7}$$

where λ is a coefficient relating to the deformation capacity varying from 5-12 according to Xu (Xu 1999), $d_{\max}$ is the maximum diameter of coarse aggregate.

2.3.2 Determination of the critical cohesive fracture toughness K_I^c

The standard Green's function (Tada *et al*. 1985) for the edge cracks with finite width of plate subjected to a pair of normal forces is used to evaluate the value of cohesive toughness. The general expression for the cohesive fracture toughness associated with cohesive stress distribution in the fictitious fracture zone for Mode I fracture is given as below:

$$K_I{}^c = \int_{a_0}^{a} 2\sigma(x) F\left(\frac{x}{a}, \frac{a}{h}\right) / \sqrt{\pi a}\, dx \tag{8}$$

where

$$F\left(\frac{x}{a}, \frac{a}{h}\right) = \frac{3.52(1 - x/a)}{(1 - a/h)^{3/2}} - \frac{4.35 - 5.28x/a}{(1 - a/h)} + \left(\frac{1.30 - 0.30(x/a)^{3/2}}{\sqrt{1 - (x/a)^2}} + 0.83 - 1.76\frac{x}{a}\right)\left(1 - \left(1 - \frac{x}{a}\right)\frac{a}{h}\right) \tag{9}$$

And $\sigma(x)$ is the cohesive force at crack length x (see Fig.3) , its expression is shown in Eqs.10 or 12.

At critical situation the value of a is taken to be a_c in Eqs.8 and 9. The integration of the Eq.8 is done by using Gauss-Chebyshev quadrature method because of existence of singularity at the integral boundary.

As shown in Fig.2, two situations at critical load, i.e., $CTOD_c \le w_s$ and $w_s \le CTOD_c \le w_c$ may arise at the notch-tip when using the bilinear softening functions. For specimens subjected to temperatures less than 120℃, the $CTOD_c$ is less than w_s; while, for temperatures higher than 120℃, the $CTOD_c$ is wider than w_s.

A. When the $CTOD_c$ corresponding to the maximum load P_{max} is less than w_s as shown Fig.2a. The distribution of cohesive stress along the fictitious fracture zone is approximated to be linear as shown in Fig.3a. The variation of cohesive stress along the fictitious fracture zone for this loading situation i.e., $a_o \le a \le a_c$ or $0 \le CTOD \le CTOD_c$ is written as:

$$\sigma(x) = \sigma(CTOD_c) + \left(f_t - \sigma(CTOD_c)\right)(x - a_0)/(a_c - a_0) \tag{10}$$

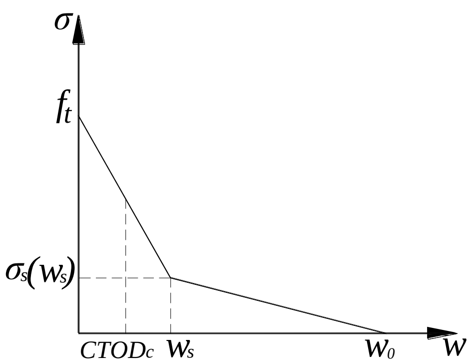

(a) When $CTOD_c \le w_s$

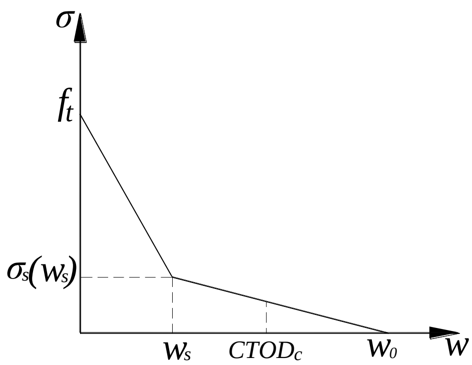

(b) When $CTOD_c > w_s$

Fig. 2 Two different situations for $CTOD_c$ and w_s

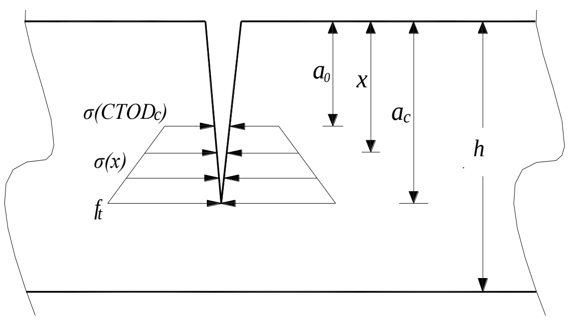

(a) The linear distribution of cohesive force

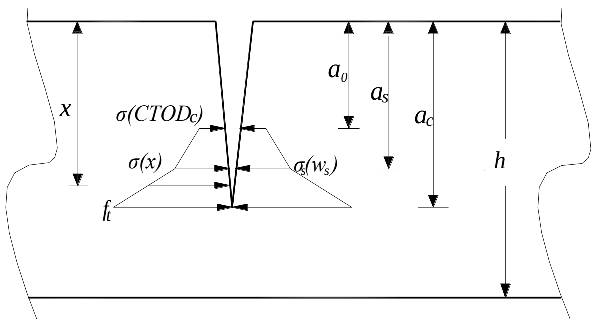

(b) The bilinear distribution of cohesive force

Fig. 3 Cohesive force distribution along the crack length at critical load where, σ ($CTOD_c$) is the critical value of cohesive stress being at the tip of initial notch. The value of σ ($CTOD_c$) is determined by using the bilinear softening function:

$$\sigma(CTOD_c) = \sigma_s(w_s) + \frac{w_s - CTOD_c}{w_s}\left(f_t - \sigma_s(w_s)\right) \tag{11}$$

The critical cohesive fracture toughness in this case is evaluated using Eqs.8 and 9.

B. When the critical $CTOD_c$ corresponding to the maximum load P_{max} is wider than w_s as shown Fig.2b. The distribution of cohesive stress along the fictitious fracture zone is approximated to be bilinear as shown in Fig.3b. The variation of cohesive stress along the fictitious fracture zone for this loading situation, also, $a_o \le a \le a_c$ or $0 \le CTOD \le CTOD_c$ is written as:

$$\begin{cases} \sigma_1(x) = \sigma(CTOD_c) + \left(\sigma_s(w_s) - \sigma(w)\right)\dfrac{(x - a_0)}{(a_s - a_0)} & a_s \le x \le a_0 \\ \sigma_2(x) = \sigma_s(w_s) + \left(f_t - \sigma_s(w_s)\right)\dfrac{(x - a_s)}{(a_c - a_s)} & a_s \le x \le a_c \end{cases} \tag{12}$$

The value of σ ($CTOD_c$) is determined by using the bilinear softening function:

$$\sigma(CTOD_c) = \frac{w_0 - CTOD_c}{w_0 - w_s}\sigma_s(w_s) \tag{13}$$

The integration limits of Eq.8 should be taken in two steps: $a_o \le x \le a_s$ for cohesive stress $\sigma_1(x)$ and $a_s \le x \le a_c$ for cohesive stress $\sigma_2(x)$ respectively. The same Green's function F(x/a, a/h) for a given effective crack extension will be determined using Eq.9. The calculated formula is listed as follows:

$$K_I{}^{c} = \int_{a_0}^{a_s} 2\sigma_1(x)F\left(\frac{x}{a_c}, \frac{a_c}{h}\right) / \sqrt{\pi a_c}\,dx + \int_{a_s}^{a_c} 2\sigma_2(x)F\left(\frac{x}{a_c}, \frac{a_c}{h}\right) / \sqrt{\pi a_c}\,dx \tag{14}$$

The effective crack length at break point a_s (shown in Fig.3b), is computed from the following nonlinear expression by substituting COD (a_s), $CMOD_c$, a_c and h:

$$COD(a_s) = CMOD_c\left(\left(1 - \frac{a_s}{a_c}\right)^2 + \left(1.018 - 1.149\frac{a_c}{h}\right)\left(\frac{a_s}{a_c} - \left(\frac{a_s}{a_c}\right)^2\right)\right)^{1/2} \tag{15}$$

where COD (a_s) is the crack opening displacement at a_s, i.e., w_s; a_c is the effective crack length (according to Eq.1) and h is the specimen height.

3. Calculation of double-*K* fracture parameters

The two parameters (K_I^{ini} and K_I^{un}) of double-K fracture criterion for wedge splitting test are determined using the linear elastic fracture mechanics formulas given in Xu (Xu and Reinhardt

1999b):

$$K(P,a)=\frac{P\times 10^{-3}}{th^{1/2}}\,f(\alpha) \tag{16}$$

$$f(\alpha)=\frac{3.675\times(1-0.12(\alpha-0.45))}{(1-\alpha)^{3/2}},\alpha=\frac{a}{h} \tag{17}$$

The empirical expression (16) is valid within 2% accuracy for, $0.2 \le \alpha \le 0.8$.

Eqs. 16 and 17 can be used in the calculation of unstable fracture toughness K_I^{un} at the tip of effective crack length a_c, in which $a = a_c$ and $P = P_{max}$. The initiation toughness K_I^{ini} is calculated when the initial cracking load, P_{ini} is known. In present paper, the P_{ini} is determined by graphical method using the starting point of non-linearity in *P-CMOD* curve described in the previous research (Yu and Lu 2014).

Generally, for the post-fire concrete specimens the value of initial fracture toughness K_I^{ini} is far less than the one of critical fracture toughness K_I^{un}, especially for higher temperatures. So much more considerations are put to the critical fracture toughness K_I^{un}. In the double-K fracture model, the following relation can be employed:

$$K_I^{\,un}=K_I^{\,ini}+K_I^{\,c} \tag{18}$$

Here, we donate the experimental value of critical fracture toughness as $K_I^{un\text{-}E}$, the analytical values of calculated from Peterson's, CEB-FIP model and Xu's softening curve as $K_I^{un\text{-}AP}$, $K_I^{un\text{-}AC}$ and $K_I^{un\text{-}AX}$, respectively. From the comparisons between $K_I^{un\text{-}E}$ and $K_I^{un\text{-}AP}$, between $K_I^{un\text{-}E}$ and $K_I^{un\text{-}AC}$, or between $K_I^{un\text{-}E}$ and $K_I^{un\text{-}AX}$, we could judge the influence of softening curves on the fracture toughness and the validation of double-*K* fracture model to the post-fire concrete.

4. Briefly experimental information

4.1 Experimental program and experimental phenomena

The experimental program is the same as the authors' previous research (Yu *et al*. 2012) and here only makes a brief introduce. Totally 50 wedge-splitting concrete specimens with the same dimensions 230 mm × 200 mm × 200 mm were implemented, the specimen geometry is shown in Fig. 4 (b = 200 mm, d = 65 mm, h = 200 mm, f = 30 mm, a_0 = 80 mm, θ = 15°). The concrete mix ratios (by weight) were Cement: Silica sand: Limestone coarse aggregate: Water = 1.00:3.44:4.39:0.80, with ordinary Portland cement, medium sand and 16mm graded coarse aggregate. The compressive strength for 28 days was 34MPa. Nine heating temperatures, ranging from 65℃ to 600℃ (T_m = 65℃, 120℃, 200℃, 300℃, 350℃, 400℃, 450℃, 500℃, 600℃), were adopted with the ambient temperature as a reference. An electric furnace with net dimensions of 300 mm × 300 mm × 900 mm was used for heating.

A universal testing machine with a maximum capacity of 1000 kN was employed to conduct the wedge splitting test. A Clip-on Extensometers was suited at the mouth of crack to measure the crack mouth opening displacement (*CMOD*) and the complete *P-CMOD* curves (shown in Fig.5) of all temperatures were obtained at a fixed testing rate of 0.4 mm/min.

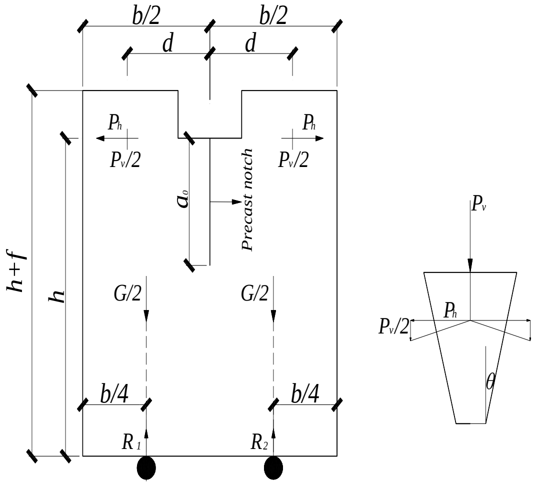

Fig. 4 The geometry of specimens

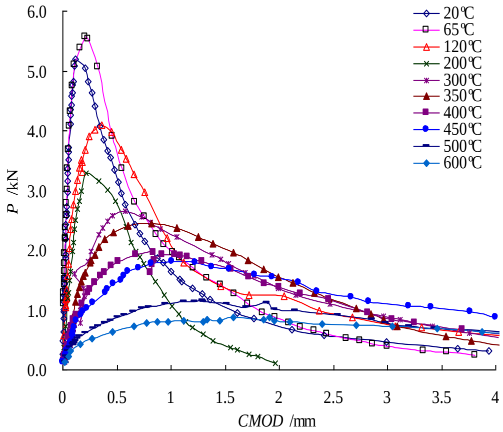

Fig. 5 P vs. $CMOD$ curves of specimens with temperatures

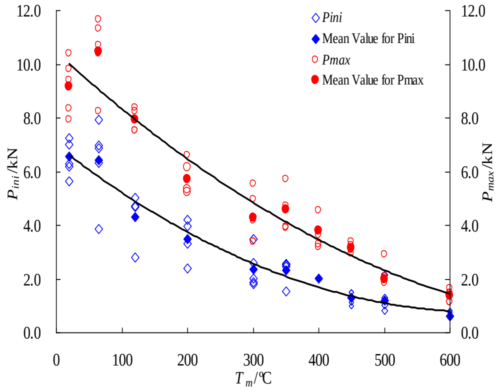

Fig. 6 Variation tendency of P_{ini} and P_{max} with T_m

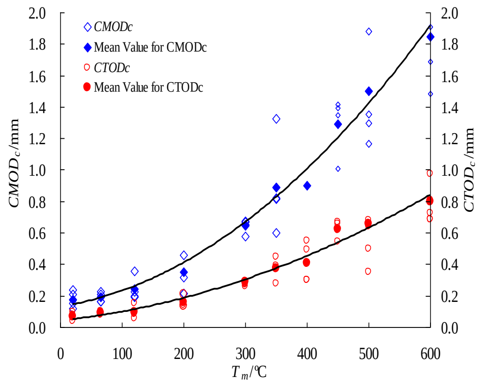

Fig. 7 Variation tendency of $CMOD_c$ and $CTOD_c$ with T_m

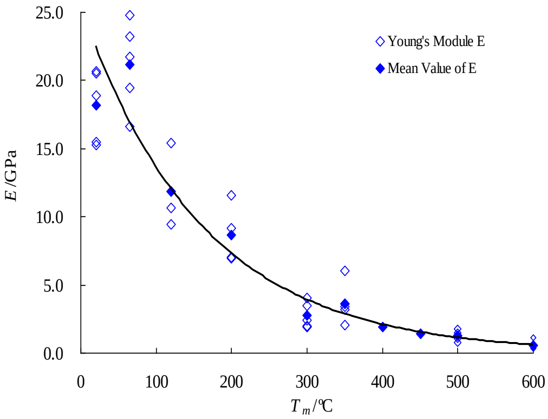

Fig. 8 Variation tendency of Young's Module E with T_m

4.2 Experimental results

Fig. 5 shows the typical complete load-displacement curves for the heating temperatures up to 600℃. The ultimate loads P_{max} decrease significantly with increasing temperatures T_m, whereas the crack mouth opening displacements (*CMOD*) increase with T_m. The initial slopes of ascending branches decrease with heating temperatures, and the curves become gradually shorter and more extended.

The recorded maximum load P_{max} and the corresponding crack mouth opening displacement $CMOD_c$ at P_{max}, the calculated crack tip opening displacement $CTOD_c$ based on Eq.15, the initial cracking load P_{ini} determined by graphical method, the calculated residual Young's modulus E based on Eq.2, and the residual fracture energy G_F are necessary to determine the double-K fracture toughness. It is found that the initial load P_{ini}, ultimate load P_{max}, the residual Young's modulus E, and the double-K fracture parameters decrease with the increasing temperatures. Whereas the $CMOD_{ini}$, $CMOD_c$, $CTOD_c$, and a_c/h increase with T_m. The G_F sustains an increase-decrease tendency with T_m with the detail explanation could be found in our previous work (Yu *et al.* 2012). Figs.6-8 show the variation tendencies of these parameters.

The average value of P_{ini} decreases from 6.55 kN at ambient temperature to 4.31 kN at 120℃, 2.37 kN at 300℃, 1.29 kN at 450℃, and finally to 0.62 kN at 600℃. And the average value of P_{max} decreases from 9.17 kN at ambient temperature to 7.92 kN at 120℃, 4.29 kN at 300℃, 3.16 kN at 450℃, and finally to 1.38 kN at 600℃, with a final drop of 85%.

$CMOD_{ini}$, $CMOD_c$ and a_c/h increase with T_m. The value of $CMOD_{ini}$ increases from 0.065 mm at ambient temperature to 0.117 mm at 200℃, 0.160 mm at 400℃, and 0.324 mm at 600℃, nearly 5 times as the ambient value. The value of $CMOD_c$ increases from 0.178 mm at ambient temperature to 0.352 mm at 200℃, 0.901 mm at 400℃, and 1.848 mm at 600℃, nearly 10 times as the ambient value.

The residual Young's modulus E drops from 18.16 GPa at ambient temperature to 11.86 GPa at 120℃, 8.68 GPa at 200℃, 2.78 GPa at 300℃, 1.48 GPa at 450℃, and finally 0.57 GPa at 600℃ with a total drop of 97%. The thermal damage induced by the high temperature greatly reduces the stiffness of concrete due to the full development of micro cracks. And obviously the tensile Young's modulus is suffered more seriously from thermal damage than the compressive Young's modulus. When the specimen subjected to tensile stress, the micro cracks become wider; while the micro cracks would close when subjected to the compressive stress and the coarse aggregates between the cracks would help to transfer the compressive stress.

5. Discussion

5.1 The variation tendency of fracture toughness

In order to express the influence of high temperature on the residual fracture toughness in detail, Fig.10 plots the tendency of the initial fracture toughness K_I^{ini} and the unstable fracture toughness K_I^{un} with the heating temperatures T_m. It is concluded that the two fractures toughness decrease monotonously with T_m because of the thermal damage induced.

The initial fracture toughness continuously decreases from 0.498 kN at room temperature to 0.269 kN at 200℃, 0.115 kN at 450℃, and finally 0.064kN at 600℃, with a significant loss of 0.434 kN or 96%. The unstable fracture toughness decreases from 1.186 kN at room temperature to 0.297 at 600℃, with a significant loss of 0.889 kN or 75%.

5.2 Influence of softening curve on fracture toughness

Fig.10 shows the comparison between the analytical and the experimental fracture toughness value, it can be seen that the values of $K_I^{un\text{-}AP}$, $K_I^{un\text{-}AC}$ and $K_I^{un\text{-}AX}$ evaluated by equation (18) of different heating temperatures have a good coincidence to the experimental values of $K_I^{un\text{-}E}$ by inserting P_{max} and $a_c = h$ into the equation (16).
From Table 1, it is known that in totally 45 effective specimens, the deviation between $K_I^{un\text{-}AP}$ and $K_I^{un\text{-}E}$ of 22 specimens is below 5%, and of 40 specimens is below 15%, accounting for 89%of total specimens. Correspondingly, 21 specimens below 5% and 38 specimens below 15% are for $K_I^{un\text{-}AC}$, and 34 specimens below 5% and 41specimens below 15% are for $K_I^{un\text{-}AX}$. The slight difference between the analytical and the experimental values further proves the validation of double-K fracture model to the post-fire concrete.

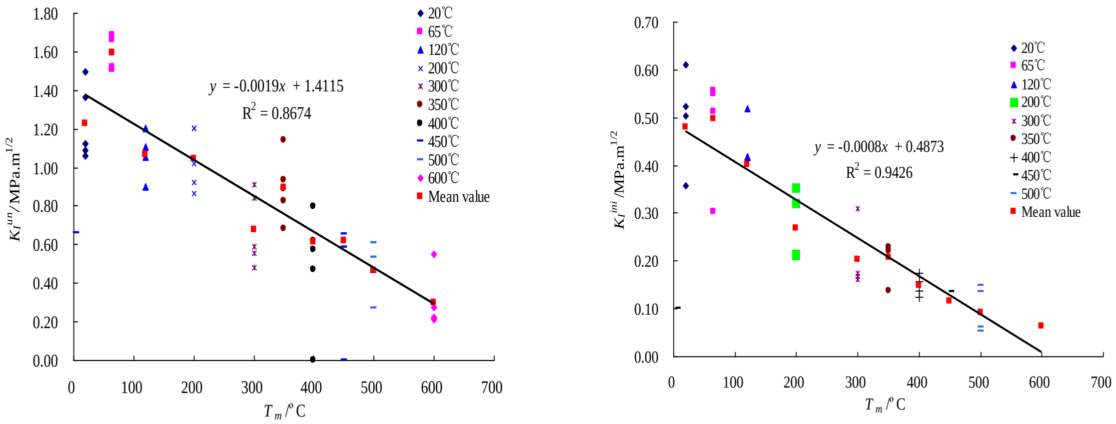

(a) Tendency of K_I^{ini} with T_m (b) Tendency of K_I^{un} with T_m

Fig. 9 Tendency of residual fracture toughness with heating temperatures T_m

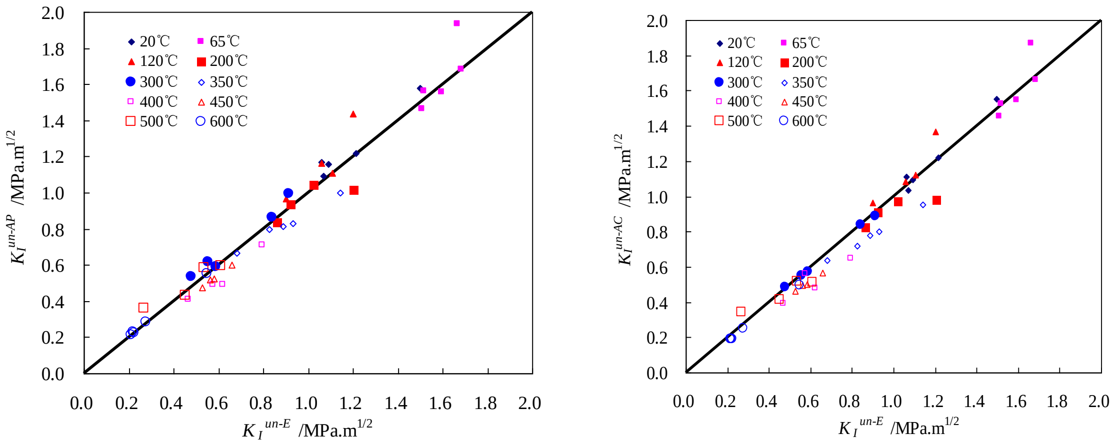

(a) Comparison between $K_I^{un\text{-}AP}$ and $K_I^{un\text{-}E}$ (b) Comparison between $K_I^{un\text{-}AC}$ and $K_I^{un\text{-}E}$

Fig. 10 Comparison between analytical and experimental fracture toughness value

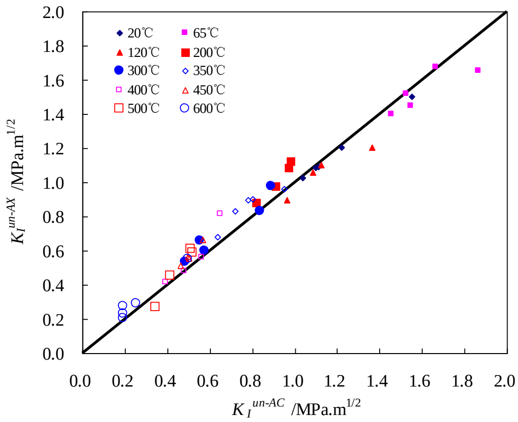

(c) Comparison between $K_I^{un\text{-}AX}$ and $K_I^{un\text{-}E}$

Fig. 10 Continued

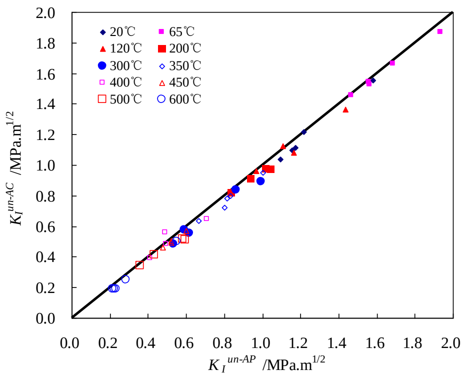

(a)

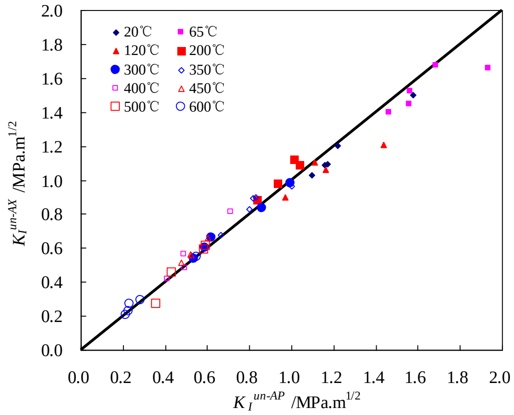

(b)

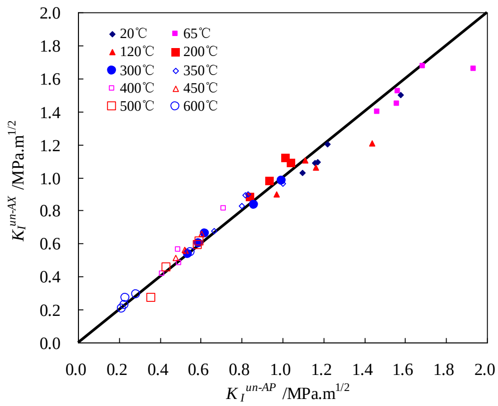

(c)

Fig. 11 Comparison the fracture toughness among $K_I^{un\text{-}AP}$, $K_I^{un\text{-}AC}$ and $K_I^{un\text{-}AX}$

Table 1 Comparison between experimental and analytical fracture toughness

	Deviation no more than 5%	Deviation no more than 10%	Deviation no more than 15%	Deviation more than 15%
Between $K_I^{un\text{-}E}$ and $K_I^{un\text{-}AP}$	22（0.49）	33（0.73）	40（0.89）	5 (11%)
Between $K_I^{un\text{-}E}$ and $K_I^{un\text{-}AC}$	21（0.47）	27（0.6）	38（0.84）	7 (16%)
Between $K_I^{un\text{-}E}$ and $K_I^{un\text{-}AX}$	34（0.75）	38（0.84）	41（0.91）	4 (9%)

5.3 Comparison among the three softening curves

Fig.11 shows the comparison between the analytical critical fracture toughness based on different softening curves. It can be concluded that the calculated values from CEB-FIP model are generally smaller than the ones obtained from Petersson's and Xu's softening curve, the detailed explanation could be found elsewhere which relates to the specific values of softening curves themselves (Yu and Lu 2014). However, it also indicates that different softening curves have no significant influence on the results of analytical fracture toughness. Such that in the future work, any of these three curves could be used to calculate the fracture parameters and be used in the analysis of post-fire concrete or concrete members without bringing obvious differences.

6. Conclusion

A comparative study on determining the residual fracture toughness associated with three bi-linear functions of the cohesive stress distribution, i.e. Peterson's softening curve, CEB-FIP Model 1990 softening curve and Xu's softening curve, using an analytical method is presented in this paper.

The validation of double-K fracture model to the post-fire concrete specimens is proved. In totally 45 effective specimens, the deviation between the analytical value $K_I^{un\text{-}AP}$ and the experimental value $K_I^{un\text{-}E}$ of 22 specimens is below 5%, and of 40 specimens is below 15%, corresponding to 21 and 38 specimens for $K_I^{un\text{-}AC}$, 34 and 41specimens for $K_I^{un\text{-}AX}$.

The calculated values of critical fracture toughness from CEB-FIP model are generally smaller than the ones obtained from Petersson's and Xu's softening curve, which relates to the specific values of softening curves. Furthermore, the comparison between the analytical fracture toughness values indicates that different softening curves have no significant influence on fracture toughness. Such that in the future work, any of these three curves could be used to calculate the fracture parameters and be used in the analysis of post-fire concrete or concrete members without bringing obvious differences.

Acknowledgment

The authors are grateful for the financial support received from the Natural Science Fund of Ch ina (Project No. 51478362 and 51378397).

Reference

Baker, G. (1996), "The effect of exposure to elevated temperatures on the fracture energy of plain concrete", *RILEM Mater. Struct.*, **29**(6), 383-388.

Bazant, Z.P. and Oh, B.H. (1983), "Crack band theory for fracture of concrete", *RILEM Mater Struct*, **16**(93), 155-177.

Bazant, Z.P. and Prat, P.C. (1988), "Effect of temperatures and humidity on fracture energy of concrete", *ACI Mater. J.*, **85**(4), 262-271.

Bazant, Z.P. and Kazemi, M.T. (1990), "Determination of fracture energy, process zone length and brittleness number from size effect, with application to rock and concrete", *Int. J. Fract.*, **44**(2), 111-131.

Bretschneider, N., Slowik, V., Villmann, B. and Mechtcherine, V. (2011), "Boundary effect on the softening curve of concrete", *Eng. Fract. Mech.*, **78**(17), 2896-2906.

Bueckner, H.F. (1970), "A novel principle for the computation of stress intensity factors", *Z. Angew. Math. Mech.*, **50**(2), 529-546.

Bulletin D' Information (1993), *CEB-Comite Euro-international du Beton-CEB-FIP Model Code 1990*, Lausanne.

Chen, H.H. and Su, R.K.L. (2013), "Tension softening curves of plain concrete", *Constr. Build. Mater.*, **44**(7), 440-451.

Glinka, G. and Shen, G. (1991). "Universal features of weight functions for cracks in Mode I", *Eng. Fract. Mech.*, **40**(6), 1135-1146.

Gopalaratnam, V.S. and Shah, S.P. (1985), "Softening response of plain concrete in direct tension", *ACI Mater. J.*, **82**(3), 310-323.

Hillerboerg, A., Modeer, M. and Peterson P.E. (1976), "Analysis of crack formation and crack growth in concrete by means of fracture mechanics and finite elements", *Cement Concrete Res.*, **6**(6), 773-782.

Hilsdorf, H.K. and Brameshuber, W. (1991), *Current Trends in Concrete Fracture Research*. Springer, Netherlands.

Hisham, A.F. and Sameer, A.H. (1997), "Variation of the fracture toughness of concrete with temperature", *Constr. Build. Mater.*, **11**(2), 105-108.

Jenq, Y.S. and Shah, S.P. (1985a), "Two parameter fracture model for concrete", *J Eng Mech*, ASCE, **111**(10), 1227-1241.

Jenq, Y.S. and Shah, S.P. (1985b), "A fracture toughness criterion for concrete", *Eng. Fract. Mech.*, **21**(5), 1055-1069.

Kumar, S. and Barai, S.V. (2012), "Size-effect of fracture parameters for crack propagation in concrete: a comparative study", *Comput. Concr.*, **9**(1), 1-19.

Kumar, S. and Barai, S.V. (2010), "Determining the double-K fracture parameters for three-point bending notched concrete beams using weight function", *Fatigue Fract. Eng. Mater Struct*, **33**(10), 645-660.

Kumar, S. and Barai, S.V. (2009), "Determining double-K fracture parameters of concrete for compact tension and wedge splitting tests using weight function", *Eng. Fract. Mech.*, **76**(7), 935-946.

Kumar, S. and Barai, S.V. (2008a), "Influence of specimen geometry and size-effect on the K_R-curve based on the cohesive stress in concrete", *Int. J. Fract.*, **152**(2), 127-148.

Kumar, S. and Barai, S.V. (2008b), "Influence of specimen geometry on determination of double-K fracture parameters of concrete: a comparative study", *Int. J. Fract*, **149**(1), 47-66.

Kwon, S.H., Zhao, Z.F. and Shah, S.P. (2008), "Effect of specimen size on fracture energy and softening curve of concrete: Part II. Inverse analysis and softening curve", *Cement Concrete Res.*, **38**(8), 1061-1069.

Nallathambi, P. and Karihaloo, B.L. (1986), "Determination of specimen-size independent fracture toughness of plain concrete", *Mag. Concr. Res.*, **38**(135), 67-76.

Nielsen, C.V. and Bicanic, N. (2003), "Residual fracture energy of high-performance and normal concrete subject to high temperatures", *RILEM Mater. Struct.*, **36**(8), 515-521.

Petersson, P.E. (1981), *Crack Growth and Development of Fracture Zones in Plain Concrete and Similar Materials*, Division of Building Materials, Lund Institute of Technology, Report TVBM-1006, Sweden.

Park, K., Paulino, H.G. and Roesler, J.R. (2008), "Determination of the kink point in the bilinear softening model for concrete", *Eng. Fract. Mech.*, **75**(13), 3806-3818.

Phillips, D.V. and Zhang, Z. (1993), "Direct tension tests on notched and un-notched plain concrete specimens", *Mag. Concr. Res.*, **45**(162), 25-35.

Prokopski, G. (1995), "Fracture toughness of concretes at high temperature", *J Mater. Sci.*, **30**(6), 1609-1612.

Reinhardt, H.W., Cornelissen, H.A.W. and Hordijk, D.A. (1986), "Tensile tests and failure analysis of concrete", *J. Struct. Eng. ASCE*, **112**(11), 2462-2477.

Roesler, J., Paulino, G.H., Park, K. and Gaedicke, C. (2007), "Concrete fracture prediction using bilinear softening", *Cement Concrete Compos.*, **29**(4), 300-312.

Tada, H., Paris, P.C. and Irwin, G. (1985), *The stress analysis of cracks handbook*. Paris Productions Incorporated, St. Louis, Paris, France.

Xu, S. and Reinhardt, H.W. (1999a), "Determination of double-K criterion for crack propagation in quasi-brittle materials, Part I: Experimental investigation of crack propagation", *Int. J. Fract.*, **98**(2), 111-149.

Xu. S and Reinhardt, H.W. (1999b), "Determination of double-K criterion for crack propagation in quasi-brittle materials, Part II: Analytical evaluating and practical measuring methods for three-point bending notched beams", *Int. J. Fract*, **98**(2), 151-177.

Xu, S. and Reinhardt, H.W. (1999c), "Determination of double-K criterion for crack propagation in quasi-brittle materials, Part III: Compact tension specimens and wedge splitting specimens", *Int. J. Fract.*, **98**(2), 179-193.

Yu, J.T., Yu, K.Q. and Lu, Z.D. (2012), "Residual fracture properties of concrete subjected to elevated temperatures", *RILEM Mater. Struct.*, **45** (8), 1155-1165.

Yu, K.Q. and Lu, Z.D. (2014), "Determining residual double-K fracture toughness of post-fire concrete using analytical and weight function method", *RILEM Mater. Struct.*, **47**(5), 839-852.

Zhang, B., Bicanic, N., Pearce, C.J. and Balabanic, G. (2000), "Residual fracture properties of normal and high-strength concrete subject to elevated temperatures", *Mag. Concr. Res.*, **52**(2), 123-136.

Zhang, B. and Bicanic, N. (2006), "Fracture energy of high-performance concrete at high temperatures up to 450ºC: the effects of heating temperatures and testing situations (hot and cold)", *Mag. Concr. Res.*, **58**(5), 277-288.

Zhang, B., Bicanic, N., Pearce, C.J. and Phillips, D.V. (2002), "Relationship between brittleness and moisture loss of concrete exposed to high temperatures", *Cement Concrete Res.*, **32**(3), 363-371.

Zhang, B., Bicanic, N., Pearce, C.J. and Balabanic, G. (2000), "Assessment of toughness of concrete subjected to elevated temperatures from complete load-displacement curve- Part I: General introduction", *ACI Mater.*, **97**(5), 550-555.

Zhang, B., Bicanic, N., Pearce, C.J. and Balabanic, G. (2000), "Assessment of toughness of concrete subjected to elevated temperatures from complete load-displacement curve- Part II: Experimental Investigation", *ACI Mater.*, **97**(5), 556-566.

CC